How Effective Are Time-Series Models for Rainfall Nowcasting? A Comprehensive Benchmark for Rainfall Nowcasting Incorporating PWV Data

Yifang Zhang, Pengfei Duan*, Henan Wang, Shengwu Xiong*,

[1]School of Computer Science and Artificial Intelligence, Wuhan University of Technology

Abstract

Rainfall nowcasting, which aims to predict precipitation within the next 0 to 3 hours, is critical for disaster mitigation and real-time response planning. However, most time series forecasting benchmarks in meteorology are evaluated on variables with strong periodicity, such as temperature and humidity, which fail to reflect model capabilities in more complex and practically meteorology scenarios like rainfall nowcasting. To address this gap, we propose ***RainfallBench***, a benchmark designed for rainfall nowcasting, a highly challenging and practically relevant task characterized by zero inflation, temporal decay, and non-stationarity, focused on predicting precipitation within the next 0 to 3 hours. The dataset is derived from five years of meteorological observations, recorded at 15-minute intervals across six essential variables, and collected from more than 12,000 GNSS stations globally. In particular, it incorporates precipitable water vapor (PWV), a crucial indicator of rainfall that is absent in other datasets. We further design specialized evaluation strategies to assess model performance on key meteorological challenges, such as multi-scale prediction and extreme rainfall events, and evaluate over 20 state-of-the-art models across six major architectures on RainfallBench. Additionally, to address the zero-inflation and temporal decay issues overlooked by existing models, we introduce ***Bi-Focus Precipitation Forecaster (BFPF)***, a plug-and-play module that incorporates domain-specific priors to enhance rainfall time series forecasting. Statistical analysis and ablation studies validate the comprehensiveness of our dataset as well as the superiority of our methodology. Code and datasets are available at https://anonymous.4open.science/r/RainfallBench-A710.

Introduction

Rainfall nowcasting, which focuses on predicting precipitation within the next 0 to 3 hours (Zhang et al. 2023; Nearing et al. 2024), plays a crucial role in disaster mitigation, flood prevention, and real-time decision-making in weather-sensitive sectors. However, current time series forecasting models in meteorology are often evaluated on variables that exhibit strong periodic patterns, such as temperature and humidity. While these benchmarks facilitate model development and comparison, they often fall short in capturing the complexity and uncertainty inherent in real-world meteorology scenarios, and do not adequately assess model performance on rainfall prediction—one of the most critical atmospheric variables. This gap raises concerns about the practical applicability and robustness of existing models.

To bridge this discrepancy, we introduce **RainfallBench**, a benchmark tailored for rainfall nowcasting — a task characterized by zero inflation, temporal decay, and non-stationarity arising from complex atmospheric dynamics. These properties pose substantial challenges to time-series models, making rainfall nowcasting a more realistic and demanding benchmark for evaluating their effectiveness in practical scenarios.

In recent years, rainfall forecasting has spurred intense activity from the deep learning community. On one hand, most precipitation nowcasting methods rely on weather radar imagery (Franch et al. 2020; Tang et al. 2023; Rivero, Patiño, and Pucheta 2015; An et al. 2025), which is effective but constrained by high costs, limited coverage, and inconsistent continuity. On the other hand, existing benchmarks for time-series forecasting models in in meteorology mainly target longer-term multivariate climate variable forecasting (Wu et al. 2021; Mouatadid et al. 2023) and do not address rainfall nowcasting needs.

In particular, when using the commonly adopted Weather dataset [1] for time series forecasting, most models adopt a multivariate prediction setting, and even in univariate settings, the target variable is typically the last column—CO_2 concentration of ambient air. As a result, the evaluation metrics derived from this dataset do not adequately reflect the capability of time series models in the context of rainfall forecasting. Moreover, effective rainfall nowcasting depends on variables strongly correlated with precipitation (e.g., PWV) over the nowcasting horizon, which are often missing from other datasets, making model development and evaluation challenging. To the best of our knowledge, **RainfallBench** is the first benchmark dedicated to rainfall nowcasting solely based on historical numerical meteorological records, explicitly incorporating PWV.

It consists of data collected from over 12,000 GNSS stations globally between 2018 and 2022, covering six key meteorological variables. All measurements are sampled at 15-minute intervals, enabling fine-grained temporal modeling.

Specifically, RainfallBench offers several distinctive characteristics that set it apart from existing rainfall forecasting

*Corresponding author.

[1]https://www.bgc-jena.mpg.de/wetter/

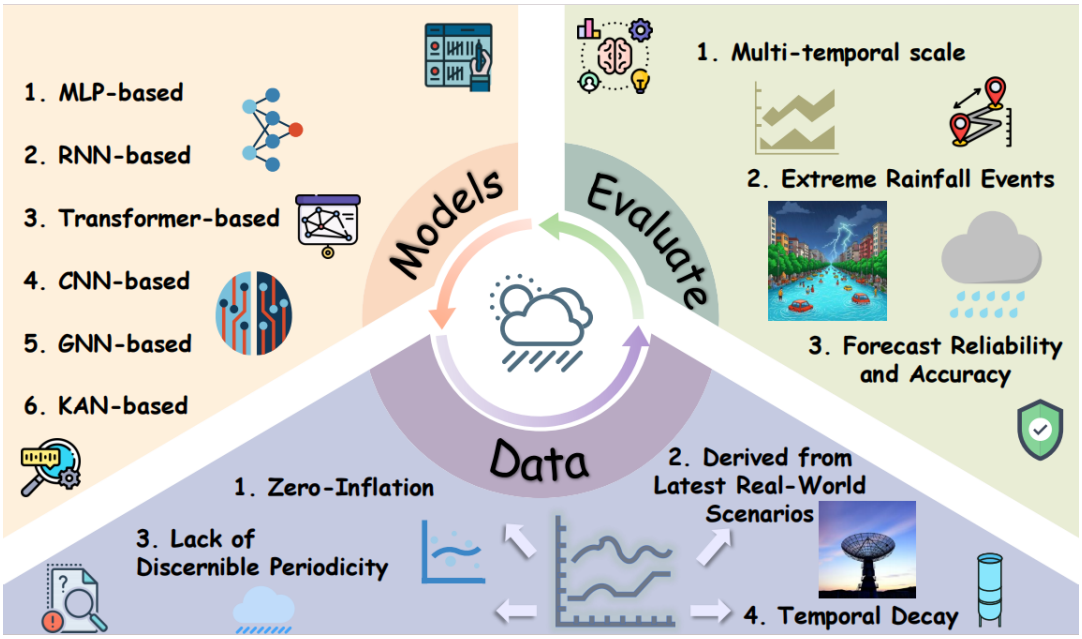

Figure 1: The Overall Architecture of RainfallBench.

datasets: **i) Integration of GNSS-Derived Atmospheric Water Vapor**: The dataset includes precipitable water vapor (PWV) derived from GNSS observations, which reflects atmospheric moisture and correlates strongly with precipitation onset, making it a key and timely indicator for short-term rainfall nowcasting (Yin et al. 2024). **ii) High-Resolution Temporal Sampling**: All variables are recorded at 15-minute intervals, enabling the capture of rapid atmospheric dynamics. This high-frequency sampling improves the suitability of the dataset for rainfall nowcasting within a 0 to 3 hours horizon. **iv) Derived from Latest Real-World Scenarios**: Our collected dataset comprises records from 2018-2022, obtained from professional meteorological observation stations, ensuring its strong practical utility.

To ensure a professional evaluation, we propose a more holistic evaluation framework, which assesses models across three key dimensions: **i) Multi-Time Scale Prediction Evaluation**: It measures a model's ability to predict rainfall at various temporal granularities. **ii) Extreme Rainfall Event Evaluation**: It focuses on a model's performance in forecasting sudden, high-intensity rainfall events. **iii) Accuracy and Reliability of Time Series Prediction**: It comprehensively considers both the precision and stability of the model's predictions. Based on this framework, we benchmark over 20 state-of-the-art deep learning models spanning various architectural families.

Through a comprehensive evaluation, we identify that existing models often overlook the zero-inflation and temporal decay characteristics, compared to the widely acknowledged non-stationarity of time series data (Liu et al. 2022, 2023b, 2025b,a). To address these limitations, we design the **BFPF** to reinforce its sensitivity to rainfall patterns and recent temporal information. Experimental results validate the effectiveness of our approach, offering a new perspective for adapting time series models to rainfall nowcasting.

In summary, our key contributions are as follows:

- **Professional Dataset for Rainfall Nowcasting:** Our benchmark is constructed from data collected at 15-minute intervals between 2018 and 2022 from over 12,000 GNSS stations globally. It covers six key variables, including PWV, and is specifically curated to support rainfall nowcasting. The dataset will be continuously updated.
- **Rainfall-Centric Evaluation Strategy:** We design a tailored evaluation strategy from a meteorological perspective, focusing on multi-scale forecasting and extreme rainfall events.
- **Novel plug-and-play Module for Rainfall Nowcasting:** We introduce the Bi-Focus Precipitation Forecaster, a plug-and-play module that explicitly addresses zero inflation and temporal decay in rainfall data, achieving state-of-the-art performance in extreme rainfall forecasting.

To facilitate subsequent data analysis and experiments, we select one representative dataset, hereafter referred to as *JFNG*, as the primary example throughout this study. Data statistics for other stations are provided in the supplementary material.

Related Works

Benchmarks for Time-Series Forecasting

FinTSB (Hu et al. 2025a) emphasizes diversity, standardization, and real-world relevance in financial forecasting. Physiome-ODE (Klötergens et al. 2025) introduces irregularly sampled ODE-based biological datasets for IMTS evaluation. Cherry-Picking (Roque et al. 2025) warns against dataset bias and calls for more representative evaluations.

TSFM-Bench and GIFT-Eval Aksu et al. (2024) assess foundation models in zero-, few-, and full-shot regimes. TFB (Qiu et al. 2024) and TSPP (Bączek et al. 2023) propose unified pipelines to ensure fair and reproducible forecasting. LargeST (Liu et al. 2023a) offers a long-term, large-scale traffic dataset with rich metadata to evaluate deep models in realistic settings.

Time-Series Models in Meteorology

PostRainBench (Tang et al. 2023) targets NWP post-processing using deep models. RainBench (de Witt et al. 2021) provides a large-scale, multi-modal benchmark using SimSat, ERA5, and IMERG for global precipitation forecasting. Rodriguez Rivero et al. (Rivero, Patiño, and Pucheta 2015) propose a neural method for short-term rainfall prediction under missing data, leveraging time series energy and the Hurst parameter. Ana et al. (An et al. 2025) provides a comprehensive review of deep learning-based precipitation forecasting methods that utilize multi-source observational data, such as radar reflectivity and satellite imagery. Compared to time-series models with observational data, radar imagery-based methods often entail limited coverage and complex preprocessing, hindering practical deployment.

Unlike benchmarks that rely on multi-modal input, RainfallBench is tailored for rainfall nowcasting, evaluating models solely on historical meteorological time series enriched with key signals such as PWV.

RainfallBench

RainfallBench is structured into three main components: the data layer, the model layer, and the evaluation layer. The overall framework is illustrated in Figure 1.

Problem Definition

We formulate rainfall nowcasting as a multivariate-to-univariate time series prediction task. Given a sequence of historical observations comprising both meteorological variables and past rainfall values, the goal is to predict future rainfall over a fixed horizon.

Formally, let the input sequence be defined as:

$$\mathbf{X} = \{\mathbf{x}_t\}_{t=1}^{T}, \quad \mathbf{x}_t \in \mathbb{R}^D$$

where $\mathbf{x}_t$ includes meteorological factors (e.g., temperature, humidity, wind) and the rainfall measurement at time t, and D denotes the number of input variables.

The target is to predict future rainfall values:

$$\mathbf{y} = \{y_{T+1}, y_{T+2}, \ldots, y_{T+H}\}, \quad y_t \in \mathbb{R}$$

where H is the prediction horizon. Notably, the output is univariate, focusing solely on future rainfall, despite the multivariate nature of the inputs.

This setting captures the practical demands of real-world rainfall forecasting, where complex environmental factors are used to infer a single but highly critical target variable.

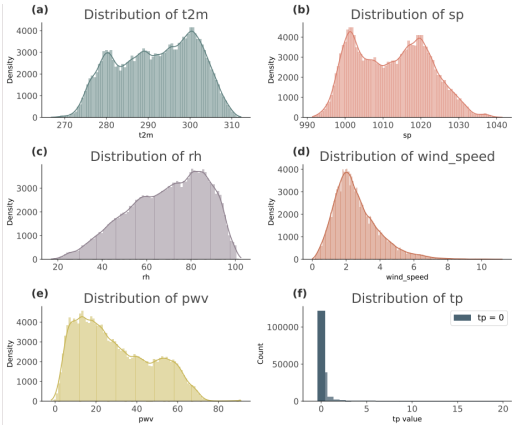

Figure 2: Variable Distributions

Datasets

Data Overview Specifically, for the *JFNG* station, we utilize a real-world meteorological dataset spanning from February 14, 2018, 00:00 to December 31, 2022, 23:00, with observations recorded every 15 minutes, totaling 171,070 time steps without missing entries. Each record consists of six variables (excluding the timestamp): five meteorological features and one target variable representing rainfall. Figure 2 illustrates the distribution of values for each variable. Specifically, the input features include:

- **t2m**: temperature at 2 meters above ground.
- **sp:** surface pressure
- **rh:** relative humidity
- **wind_speed:** wind speed.
- **PWV:** precipitable water vapor, retrieved by inverting GNSS signal delays based on their proportional relationship with atmospheric water vapor.
- **tp:** total precipitation (target), obtained from ERA5 reanalysis data.

Correlation Analysis To explore inter-variable dependencies in the RainfallBench dataset, we perform a correlation analysis using three standard metrics: Pearson, Kendall, and Spearman coefficients. The resulting matrices (Figure 3) reveal both linear and monotonic relationships.

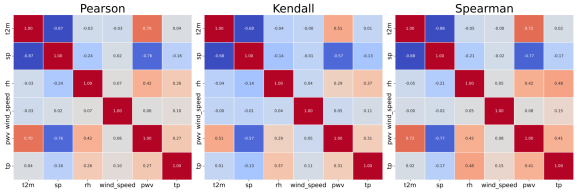

Figure 3: Pairwise correlation matrices among meteorological variables and precipitation in the RainfallBench dataset, computed using (a) Pearson, (b) Kendall, and (c) Spearman coefficients.

Across all correlation matrices, PWV shows the strongest positive correlation with tp (e.g., a Pearson coefficient of

0.27), highlighting its value as an informative feature for short-term rainfall prediction. In contrast, variables like t2m and sp exhibit weak or negative correlations, indicating limited relevance at nowcasting timescales. Since rainfall nowcasting focuses on the next 0 to 3 hours, model performance hinges on features that reflect rapid and physically meaningful atmospheric changes. Among them, PWV emerges as the most reliable indicator of imminent rainfall, making its inclusion essential in both data selection and model design. Moreover, numerous meteorological studies have observed that once PWV exceeds a certain threshold, the probability of precipitation increases significantly (Deng et al. 2021; Papée and Montefinale 1961).

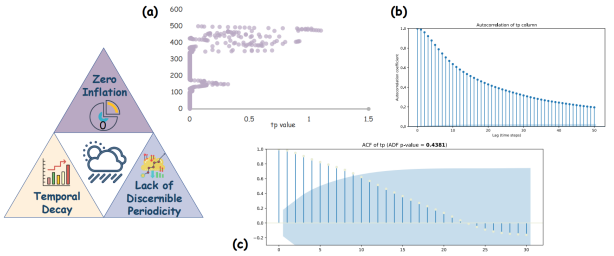

Figure 4: Analysis of Data Properties in RainfallBench

Analysis of Data Properties RainfallBench introduces three key properties that distinguish it from standard time series benchmarks: (i) zero inflation, (ii) temporal dependency decay, and (iii) non-stationarity. We now analyze each property and its modeling implications.

Zero Inflation: The majority of target values are zeros, reflecting the sparse and event-driven nature of rainfall. This sparsity undermines conventional modeling assumptions that rely on frequent signal continuity. Figure 4(a) shows the distribution of 500 randomly sampled records. It is evident that the majority have a tp value of 0. In total, there are 121,572 such records, accounting for 71% of the entire dataset.

Temporal Decay: When using historical rainfall time series to predict future values, the contributions of past observations vary over time. Typically, more recent data have a stronger influence on the prediction, while the relevance decreases as the time gap widens—an effect we refer to as temporal decay.

We characterize temporal decay via the lag-k autocorrelation function $\rho(k)$, which quantifies the dependence between current and past rainfall values. Empirically, $\rho(k)$ exhibits an approximately exponential decay:

$$\rho(k) \approx e^{-\lambda k}, \quad \lambda > 0 \tag{1}$$

indicating that recent observations carry more predictive information.

This characteristic aligns with the physical nature of rainfall, which tends to evolve gradually rather than starting or stopping abruptly. As shown in the autocorrelation analysis in Figure 4(b), this temporal decay pattern is clearly observable.

Non-Stationarity: A time series $\{x_t\}_{t=1}^{T}$ is stationary if its mean, variance, and autocovariance remain constant over time. However, rainfall sequences exhibit strong non-stationarity, particularly in nowcasting contexts, due to fast-changing weather dynamics that lead to rapid shifts in their statistical characteristics. To verify this, we apply the Augmented Dickey-Fuller (ADF) test on a randomly selected segment of 120 values. The test is based on the regression:

$$\Delta x_t = \alpha + \beta t + \gamma x_{t-1} + \sum_{i=1}^{p} \delta_i \Delta x_{t-i} + \varepsilon_t \tag{2}$$

where $\Delta x_t = x_t - x_{t-1}$ is the first-order difference, γ measures the strength of the unit root, and ε_t is white noise. ADF tests the null hypothesis $H_0 : \gamma = 0$ indicates non-stationarity (unit root exists). The resulting p-value of 0.4381 (Figure 4(c)) is far above the standard 0.05 significance threshold, failing to reject H_0. This confirms the non-stationary nature of the rainfall sequence.

These properties rarely co-occur in other time series datasets, making RainfallBench a uniquely challenging benchmark. It can expose limitations in existing architectures and call for more specialized, domain-adapted solutions.

Comparison Baselines

To ensure a comprehensive benchmark evaluation, we selected 20 models spanning commonly used architectures, including MLP-based, CNN/TCN-based, RNN-based, GNN-based, KAN-based, and Transformer-based designs. To maintain both relevance and rigor, all selected models are state-of-the-art methods proposed in top-tier AI conferences within the past four years. Details of the selected models are summarized in Table 1.

Evaluation Strategy

Multi-Temporal Scale Evaluation. We evaluate model performance under multiple temporal configurations, considering both the input history length and the forecasting horizon. Formally, we define the set of input lengths as

$$\mathcal{L}_{\text{in}} = \{24, 48\}$$

and the set of output lengths (forecasting horizons) as

$$\mathcal{L}_{\text{out}} = \{4, 6, 8, 10, 12\}$$

corresponding to 1 to 3 hour forecasts in the nowcasting task (15-minute resolution). Each model is evaluated on all combinations from the Cartesian product $\mathcal{L}_{\text{in}} \times \mathcal{L}_{\text{out}}$.

For each setting, we compute both the Mean Squared Error (MSE) and Mean Absolute Error (MAE) between the predicted rainfall sequence $\hat{y}_{1:L_{\text{out}}}$ and the ground truth sequence $y_{1:L_{\text{out}}}$, defined as:

$$\text{MSE} = \frac{1}{L_{\text{out}}} \sum_{t=1}^{L_{\text{out}}} (\hat{y}_t - y_t)^2 \tag{3}$$

$$\text{MAE} = \frac{1}{L_{\text{out}}} \sum_{t=1}^{L_{\text{out}}} |\hat{y}_t - y_t| \tag{4}$$

Accuracy and Reliability Evaluation. Two separate leaderboards are reported accordingly: one for average MSE-based ranking and the other for average MAE-based ranking

across all input-output configurations, providing a comprehensive view of each model's performance in terms of both accuracy and error scale sensitivity.

Extreme Rainfall Evaluation. Accurate extreme rainfall forecasting is vital for disaster mitigation. In RainfallBench, we follow the T/CMSA 0013-2019 standard [2], under which extreme rainfall is defined as any 15-minute period with precipitation exceeding 2mm. We label these intervals and evaluate models using MSE and MAE computed only on them.

$$\text{MSE}_{\text{extreme}} = \frac{1}{|E|} \sum_{t \in E} (\hat{y}_t - y_t)^2 \tag{5}$$

$$\text{MAE}_{\text{extreme}} = \frac{1}{|E|} \sum_{t \in E} |\hat{y}_t - y_t| \tag{6}$$

where E denotes the set of time steps labeled as extreme rainfall.

Bi-Focus Precipitation Forecaster

Motivation

Our benchmark shows that while existing time series models often consider non-stationarity, they struggle with rainfall nowcasting due to two overlooked domain-specific challenges: zero inflation and temporal decay.

To address the challenges in precipitation forecasting, we propose the BFPF, a plug-and-play module for transformer-based models. It consists of two key components: **Non-Zero Focus** and **Temporal Focus**, as illustrated in Figure 5. The Non-Zero Focus module mitigates distractions caused by non-rainy periods, while the Temporal Focus module emphasizes temporally proximate context.

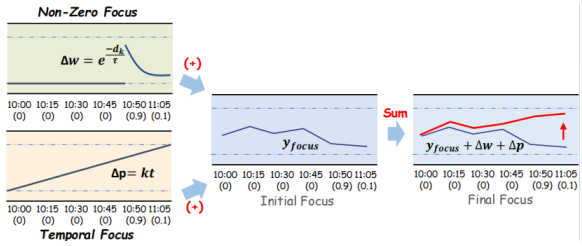

Figure 5: Bi-Focus Precipitation Forecaster

Non-Zero Focus

The Non-Zero Focus module is designed to mitigate the common challenge in rainfall forecasting where input sequences are dominated by zeros, causing the model to overlook sparse but critical non-zero values. In precipitation data, rainfall events are infrequent yet hydrologically significant. Treating zero and non-zero values equally will dilute the model's attention to meaningful patterns.

To address this, the Non-Zero Focus enhances the model's ability to detect sudden rainfall spikes within extended dry periods. It consists of two components: a Non-Zero Context Encoding module that adjusts attention based on value significance, and a Non-Zero Feature Modulation module that reinforces focus on non-zero inputs.

Non-Zero Context Encoding. To guide the attention mechanism toward informative, non-zero values, we introduce a distance-based weighting strategy that quantitatively measures each position's proximity to the nearest zero. Specifically, for each time step t in the input sequence, we compute the minimal distance to any zero-valued entry:

$$d_t = \begin{cases} +\infty, & \text{if } x_t = 0 \\ \min\left(|t - z_l|,\ |z_r - t|\right), & \text{otherwise} \end{cases} \tag{7}$$

where z_l and z_r denote the indices of the nearest zero positions to the left and right of t, respectively. If no zero exists in a given direction, a large sentinel value is used to preserve numerical stability.

The resulting distance matrix $\mathbf{D} \in \mathbb{R}^{B \times L}$ is computed efficiently using a masked cumulative maximum over token positions.

Non-Zero Feature Modulation. To further refine the model's sensitivity to informative input regions, we introduce a zero-proximity attention bias that adjusts attention scores based on each key's distance to the nearest zero.

Given the previously computed distance matrix $\mathbf{D} \in \mathbb{R}^{B \times L_K}$, we define a proximity weight as:

$$w_k = \exp\left(-\frac{d_k}{\tau}\right) \tag{8}$$

where d_k is the distance from position k to its nearest zero, and τ is a temperature hyperparameter controlling decay sharpness.

These weights are broadcasted and aligned to the attention score tensor $\mathbf{S} \in \mathbb{R}^{B \times H \times L_Q \times L_K}$, and the scores are modulated as:

$$\tilde{\mathbf{S}} = \mathbf{S} + \lambda \cdot \mathbf{W} \tag{9}$$

where λ is a learned scaling factor and $\mathbf{W}$ is the reshaped zero proximity weight matrix. This additive bias encourages the model to assign greater attention to non-zero entries, particularly those representing sudden rainfall onsets, thereby enhancing its focus on rare but meaningful precipitation events.

Temporal Focus

To enhance the attention mechanism with positional awareness, we introduce a linearly increasing positional bias to the original attention scores $\mathbf{S} \in \mathbb{R}^{B \times H \times L_Q \times L_K}$, where L_K is the length of the key sequence. The positional bias vector $\mathbf{p} \in \mathbb{R}^{L_K}$ is defined as:

$$\mathbf{p} = \alpha \cdot \left[\frac{0}{L_K}, \frac{1}{L_K}, \ldots, \frac{L_K - 1}{L_K}\right] \tag{10}$$

where α is a learnable scaling factor. This bias is broadcasted to match the shape of $\mathbf{S}$ and added to the attention scores element-wise:

$$\tilde{\mathbf{S}}_{b,h,i,j} = \mathbf{S}_{b,h,i,j} + \mathbf{p}_j \tag{11}$$

[2] https://www.chinamsa.org/

Table 1: Comparison of state-of-the-art methods. The red indicates the best-performing model, while the pink highlights the second-best.

Methods	Publication	24(4)		24(6)		24(8)		24(10)		24(12)		48(4)		48(6)		48(8)		48(10)		48(12)	
		MSE	MAE	MSE	MAE	MSE	MAE	MSE	MAE	MSE	MAE	MSE	MAE	MSE	MAE	MSE	MAE	MSE	MAE	MSE	MAE
MLP-based																					
DLinear (Zeng et al. 2023)	AAAI 2023	0.0099	0.0247	0.0189	0.0361	0.0282	0.0463	0.0371	0.0561	0.0465	0.0658	0.0099	0.0243	0.0188	0.0358	0.0281	0.0461	0.0370	0.0550	0.0450	0.0631
Koopa (Liu et al. 2023b)	NIPS 2023	0.0447	0.1859	0.0552	0.1928	0.0703	0.2012	0.0804	0.2054	0.0893	0.2102	0.0439	0.1833	0.0530	0.1884	0.0633	0.1946	0.0727	0.2006	0.0822	0.2045
TimeMixer (Wang et al. 2024a)	ICLR 2024	0.1616	0.2332	0.1096	0.2214	0.0989	0.2168	0.3193	0.2654	0.1884	0.2633	0.0392	0.1770	0.0627	0.1985	0.6356	0.3574	0.0721	0.1996	0.0796	0.2019
FilterTS (Wang et al. 2025b)	AAAI 2025	0.0215	0.0738	0.0323	0.0841	0.0546	0.1738	0.0517	0.0907	0.0640	0.1266	0.0233	0.1018	0.0404	0.1555	0.0417	0.0983	0.0519	0.1019	0.0736	0.1889
RNN-based																					
SegRNN (Lin et al. 2023)	Arxiv 2023	0.0098	0.0239	0.0201	0.0390	0.0277	0.0440	0.0379	0.0502	0.0453	0.0548	0.0086	0.0229	0.0168	0.0323	0.0252	0.0428	0.0335	0.0449	0.0435	0.0592
xLSTM (Beck et al. 2025)	NIPS 2024	0.0104	0.0318	0.0183	0.0474	0.0280	0.0491	0.0360	0.0596	0.0451	0.0662	0.0096	0.0293	0.0191	0.0442	0.0290	0.0503	0.0362	0.0635	0.0466	0.0692
P-sLSTM (Kong et al. 2025)	AAAI 2025	0.0083	0.0228	0.0163	0.0325	0.0242	0.0369	0.0328	0.0469	0.0401	0.0515	0.0081	0.0198	0.0163	0.0296	0.0262	0.0526	0.0333	0.0454	0.0413	0.0532
TCN&CNN-based																					
TimesNet (Wu et al. 2023)	ICLR 2023	0.0482	0.1873	0.0560	0.1938	0.0720	0.2008	0.0845	0.2071	0.0953	0.2113	0.0482	0.1839	0.0618	0.1924	0.0753	0.1998	0.0892	0.2047	0.0981	0.2096
TimeMixer++ (Wang et al. 2025a)	ICLR 2025	0.0406	0.1747	0.0558	0.1879	0.0644	0.1925	0.0773	0.1995	0.0875	0.2058	0.0416	0.1748	0.0513	0.1824	0.0651	0.1917	0.0751	0.1973	0.0850	0.2041
xPatch (Stitsyuk and Choi 2025)	AAAI 2025	0.0413	0.1806	0.0487	0.1758	0.0587	0.1804	0.0718	0.1982	0.0795	0.1828	0.0266	0.1307	0.0512	0.1870	0.0603	0.1922	0.0691	0.1959	0.0612	0.1050
GNN-based																					
MSGNet (Cai et al. 2024)	AAAI 2024	0.0484	0.1867	0.0607	0.1939	0.0726	0.1998	0.0840	0.2059	0.0965	0.2107	0.0477	0.1825	0.0599	0.1898	0.0720	0.1961	0.0875	0.2027	0.0967	0.2070
TimeFilter (Hu et al. 2025b)	ICML 2025	0.0409	0.1812	0.0509	0.1884	0.0630	0.1942	0.0727	0.2004	0.0841	0.2058	0.0383	0.1757	0.0480	0.1827	0.0570	0.1890	0.0670	0.1951	0.0753	0.1991
KAN-based																					
TimeKAN (Huang et al. 2025)	ICLR 2025	0.0425	0.1834	0.0527	0.1912	0.0649	0.1979	0.0751	0.2032	0.0851	0.2074	0.0406	0.1801	0.0499	0.1857	0.0599	0.1924	0.0698	0.1981	0.0806	0.2038
MMK (Han et al. 2024)	Arxiv 2024	0.0275	0.0178	0.0407	0.0361	0.0511	0.0553	0.0612	0.0765	0.0694	0.0959	0.0307	0.0197	0.0480	0.0433	0.0590	0.0667	0.0612	0.0727	0.0748	0.1020
Transformer-based																					
Informer (Zhou et al. 2021)	AAAI 2021	0.0093	0.0281	0.0176	0.0365	0.0298	0.0471	0.0358	0.0536	0.0555	0.0738	0.0102	0.0262	0.0191	0.0399	0.0270	0.0440	0.0347	0.0522	0.0462	0.0633
PatchTST (Nie et al. 2023)	ICLR 2023	0.0429	0.1823	0.0540	0.1907	0.0688	0.1997	0.0780	0.2039	0.0886	0.2081	0.0411	0.1774	0.0521	0.1874	0.0608	0.1925	0.0724	0.1955	0.0819	0.2011
iTransformer (Liu et al. 2024)	ICLR 2024	0.0411	0.1752	0.0512	0.1832	0.0647	0.1906	0.0758	0.1973	0.0876	0.2028	0.0395	0.1729	0.0505	0.1804	0.0641	0.1920	0.0742	0.1966	0.0886	0.2038
TimeXer (Wang et al. 2024b)	NIPS 2024	0.0584	0.1879	0.0719	0.1969	0.0862	0.2042	0.0950	0.2085	0.1043	0.2149	0.0413	0.1780	0.0924	0.1984	0.0617	0.1913	0.0736	0.1975	0.0801	0.2017
PPDformer (Wan et al. 2025)	ICASSP 2025	0.0222	0.0790	0.0325	0.0855	0.0449	0.0927	0.0558	0.0990	0.0668	0.1067	0.0246	0.0848	0.0492	0.1765	0.1765	0.1000	0.0803	0.2011	0.0850	0.2051
Informer(with BFPF)	Ours	0.0104	0.0276	0.0176	0.0323	0.0263	0.0428	0.0392	0.0525	0.0428	0.0531	0.0093	0.0231	0.0172	0.0355	0.0263	0.0404	0.0341	0.0500	0.0425	0.0593

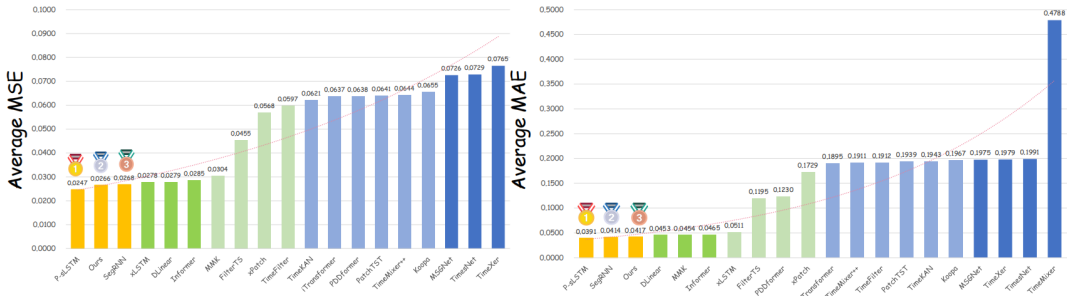

Figure 6: Model ranking based on average performance. The left panel shows the ranking by average MSE, while the right panel shows the ranking by average MAE.

where b, h, i, j index the batch, head, query position, and key position respectively. By explicitly injecting positional information, the model improves its ability to capture the relative ordering of keys, thereby enhancing positional sensitivity in attention computation.

Experiments

Experiment Setup

All experiments are conducted on an NVIDIA H100 80GB GPU. To ensure evaluation consistency, all results are computed using de-normalized actual rainfall values. For robustness, each experiment is repeated three times, and the average performance is reported as the final result. The datasets were split into training, validation, and test sets in a 7:1:2 ratio.

Experiment Results

Comprehensive forecasting results are listed in Table 1 with the best in red and the second in pink. The lower MSE/-MAE indicates the more accurate prediction result. Surprisingly, RNN-based models achieve consistently strong results, with P-sLSTM demonstrating the best overall performance across all experimental settings. Informer with our BFPF outperforms all Transformer-based counterparts, achieving the best performance under the extreme rainfall setting among all baselines.

Then, our analysis of the experimental results is guided by the following five research questions:

RQ1: How do different model architectures perform in rainfall nowcasting, and which type achieves the best results? (***Forecast Reliability and Accuracy Evaluation***)

RQ2: How does model performance vary with changes in forecasting horizon and predict length? (***Multi-temporal scale Evaluation***)

RQ3: How do different models perform for extreme rainfall forecasting? (***Extreme Rainfall Evaluation***)

RQ4: Does Incorporating PWV Significantly Enhance Rainfall Nowcasting?

RQ5: Do our proposed Bi-Focus Precipitation Forecaster improve the performance of Transformer-based models?

RQ1: Forecast Reliability and Accuracy Evaluation

As shown in Figure 6, two of the top three models are RNN-based, suggesting that RNNs are particularly well-suited for rainfall nowcasting. This is largely due to the nature of our RainfallBench dataset, which features high zero-inflation and rapid temporal decay—properties that favor models with strong short-term memory. RNNs, with their ability to emphasize recent inputs and handle sparse, irregular sequences, align well with these data characteristics. This explains why models like P-sLSTM consistently outperform others in our benchmark.

RQ2: Multi-temporal scale Evaluation

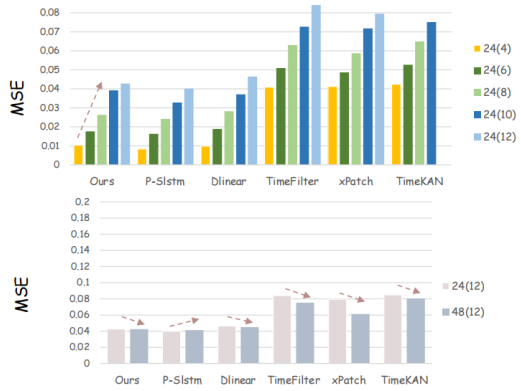

Figure 7: Model Performance Comparison Across Multiple Temporal Scales (MSE).

To ensure a fair and comprehensive evaluation, we selected representative models from six widely-used architectural families in time-series forecasting.

We consider two evaluation settings. In the first setting, we fix the input length to 24 steps and vary the forecast horizon. As expected, model errors increase with longer prediction lengths. Among all models, P-sLSTM achieves the best performance, closely followed by our model. Both significantly outperform baseline models, whose errors grow more rapidly.

In the second setting, we fix the output length to 12 steps and vary the input length (24 vs. 48). We observe that, for most models, increasing the input horizon leads to lower MSE, indicating that a longer historical context improves forecasting performance.

RQ3: Extreme Rainfall Evaluation

As shown in Figure 8, our proposed model achieves the best performance in extreme rainfall prediction, attributed to the BFPF's enhanced capability in capturing sparse signals. Interestingly, compared with general settings (Figure 6), we observe consistently higher MSE under extreme rainfall conditions, revealing the limitations of existing models and the need for advances in extreme rainfall forecasting. Comprehensive results can be found in Supplementary Material.

RQ4: Effect Analysis of PWV

To verify the effectiveness of the PWV variable in rainfall nowcasting, we train our proposed model using datasets with

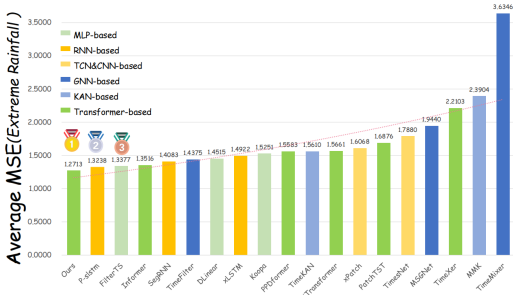

Figure 8: Model Performance on Extreme Rainfall Prediction.

(w/) and without (w/o) PWV. As shown in Table 2, incorporating PWV significantly reduces nowcasting errors, confirming both its importance for the task and the necessity of including it in RainfallBench.

Table 2: Ablation analysis of PWV

Module	48(4)		48(6)		48(8)		48(10)		48(12)	
	MSE	MAE	MSE	MAE	MSE	MAE	MSE	MAE	MSE	MAE
Ours(w/o PWV)	0.0094	0.0281	0.0194	0.0370	0.0272	0.0461	0.0345	0.0462	0.0428	0.0530
Ours(w/ PWV)	0.0093	0.0231	0.0172	0.0355	0.0263	0.0404	0.0341	0.0500	0.0425	0.0593

RQ5: Effect Analysis of Bi-Focus Precipitation Forecaster

Our ablation study in Table 3 demonstrates that incorporating the proposed BFPF significantly enhances the Transformer's performance. Incorporating either module individually yields noticeable gains over the baseline, and combining both achieves the best results across multiple forecast horizons. This highlights the importance of customizing attention mechanisms to better model rainfall-specific temporal patterns, thereby enhancing the effectiveness of Transformer models in this task.

Table 3: Ablation analysis of Non-zero&Temporal Focus

Module		48(4)		48(6)		48(8)		48(10)		48(12)	
Non-zero Focus	Temporal Focus	MSE	MAE	MSE	MAE	MSE	MAE	MSE	MAE	MSE	MAE
✗	✗	0.0102	0.0262	0.0191	0.0399	0.0270	0.0440	0.0347	0.0522	0.0462	0.0633
✗	✓	0.0093	0.0238	0.0181	0.0363	0.0271	0.0419	0.0342	0.0534	0.0455	0.0621
✓	✗	0.0091	0.0257	0.0197	0.0446	0.0254	0.0460	0.0341	0.0565	0.0472	0.0621
✓	✓	0.0093	0.0231	0.0172	0.0355	0.0263	0.0404	0.0341	0.0500	0.0425	0.0593

Conclusion

We introduce RainfallBench, the first benchmark tailored for rainfall nowcasting, explicitly integrating PWV as a key input. Evaluating over 20 state-of-the-art models, we uncover key limitations of general-purpose forecasters. To address these, we propose the Bi-Focus Precipitation Forecaster, a plug-and-play module that embeds rainfall-specific inductive biases. Results show that such domain-aware designs significantly enhance forecasting accuracy.

Future directions include exploring more effective utilization of the PWV variable, improving the model's capability in forecasting extreme events and exploring model transferability across stations.

References

Aksu, T.; Woo, G.; Liu, J.; Liu, X.; Liu, C.; Savarese, S.; Xiong, C.; and Sahoo, D. 2024. GIFT-Eval: A Benchmark for General Time Series Forecasting Model Evaluation. In *NeurIPS Workshop on Time Series in the Age of Large Models*.

An, S.; Oh, T.-J.; Sohn, E.; and Kim, D. 2025. Deep learning for precipitation nowcasting: A survey from the perspective of time series forecasting. *Expert Systems with Applications*, 268: 126301.

Bączek, J.; Zhylko, D.; Titericz, G.; Darabi, S.; Puget, J.-F.; Putterman, I.; Majchrowski, D.; Gupta, A.; Kranen, K.; and Morkisz, P. 2023. TSPP: A unified benchmarking tool for time-series forecasting. *arXiv preprint arXiv:2312.17100*.

Beck, M.; Pöppel, K.; Spanring, M.; Auer, A.; Prudnikova, O.; Kopp, M.; Klambauer, G.; Brandstetter, J.; and Hochreiter, S. 2025. xLSTM: Extended Long Short-Term Memory. *Advances in Neural Information Processing Systems*, 37: 107547–107603.

Cai, W.; Liang, Y.; Liu, X.; Feng, J.; and Wu, Y. 2024. Msgnet: Learning multi-scale inter-series correlations for multivariate time series forecasting. In *Proceedings of the AAAI Conference on Artificial Intelligence*, volume 38, 11141–11149.

de Witt, C. S.; Tong, C.; Zantedeschi, V.; De Martini, D.; Kalaitzis, A.; Chantry, M.; Watson-Parris, D.; and Bilinski, P. 2021. RainBench: Towards data-driven global precipitation forecasting from satellite imagery. In *Proceedings of the AAAI Conference on Artificial Intelligence*, volume 35, 14902–14910.

Deng, L.; Yang, F.; Chen, X.; He, F.; Liu, Q.; Zhang, B.; Zhang, C.; Wang, K.; Liu, N.; Ren, A.; et al. 2021. Lenghu on the Tibetan Plateau as an astronomical observing site. *Nature*, 596(7872): 353–356.

Franch, G.; Maggio, V.; Coviello, L.; Pendesini, M.; Jurman, G.; and Furlanello, C. 2020. TAASRAD19, a high-resolution weather radar reflectivity dataset for precipitation nowcasting. *Scientific Data*, 7(1): 234.

Han, X.; Zhang, X.; Wu, Y.; Zhang, Z.; and Wu, Z. 2024. Kan4tsf: Are kan and kan-based models effective for time series forecasting? *arXiv preprint arXiv:2408.11306*.

Hu, Y.; Li, Y.; Liu, P.; Zhu, Y.; Li, N.; Dai, T.; Xia, S.-t.; Cheng, D.; and Jiang, C. 2025a. Fintsb: A comprehensive and practical benchmark for financial time series forecasting. *arXiv preprint arXiv:2502.18834*.

Hu, Y.; Zhang, G.; Liu, P.; Lan, D.; Li, N.; Cheng, D.; Dai, T.; Xia, S.-T.; and Pan, S. 2025b. TimeFilter: Patch-Specific Spatial-Temporal Graph Filtration for Time Series Forecasting. *Forty-Second International Conference on Machine Learning*.

Huang, S.; Zhao, Z.; Li, C.; and Bai, L. 2025. TimeKAN: KAN-based Frequency Decomposition Learning Architecture for Long-term Time Series Forecasting.

Klötergens, C.; Yalavarthi, V. K.; Scholz, R.; Stubbemann, M.; Born, S.; and Schmidt-Thieme, L. 2025. PhysiomeODE: A Benchmark for Irregularly Sampled Multivariate Time Series Forecasting Based on Biological ODEs. *arXiv preprint arXiv:2502.07489*.

Kong, Y.; Wang, Z.; Nie, Y.; Zhou, T.; Zohren, S.; Liang, Y.; Sun, P.; and Wen, Q. 2025. Unlocking the power of lstm for long term time series forecasting. In *Proceedings of the AAAI Conference on Artificial Intelligence*, volume 39, 11968–11976.

Lin, S.; Lin, W.; Wu, W.; Zhao, F.; Mo, R.; and Zhang, H. 2023. Segrnn: Segment recurrent neural network for long-term time series forecasting. *arXiv preprint arXiv:2308.11200*.

Liu, P.; Wu, B.; Hu, Y.; Li, N.; Dai, T.; Bao, J.; and Xia, S.-T. 2025a. TimeBridge: Non-Stationarity Matters for Long-term Time Series Forecasting. In *Forty-second International Conference on Machine Learning*.

Liu, Q.; Xu, C.; Jiang, W.; Wang, K.; Ma, L.; and Li, H. 2025b. TimeStacker: A Novel Framework with Multilevel Observation for Capturing Nonstationary Patterns in Time Series Forecasting. In *Forty-second International Conference on Machine Learning*.

Liu, X.; Xia, Y.; Liang, Y.; Hu, J.; Wang, Y.; Bai, L.; Huang, C.; Liu, Z.; Hooi, B.; and Zimmermann, R. 2023a. Largest: A benchmark dataset for large-scale traffic forecasting. *Advances in Neural Information Processing Systems*, 36: 75354–75371.

Liu, Y.; Hu, T.; Zhang, H.; Wu, H.; Wang, S.; Ma, L.; and Long, M. 2024. iTransformer: Inverted Transformers Are Effective for Time Series Forecasting. In *The Twelfth International Conference on Learning Representations*.

Liu, Y.; Li, C.; Wang, J.; and Long, M. 2023b. Koopa: Learning non-stationary time series dynamics with koopman predictors. *Advances in neural information processing systems*, 36: 12271–12290.

Liu, Y.; Wu, H.; Wang, J.; and Long, M. 2022. Non-stationary transformers: Exploring the stationarity in time series forecasting. *Advances in neural information processing systems*, 35: 9881–9893.

Mouatadid, S.; Orenstein, P.; Flaspohler, G.; Oprescu, M.; Cohen, J.; Wang, F.; Knight, S.; Geogdzhayeva, M.; Levang, S.; Fraenkel, E.; et al. 2023. SubseasonalclimateUSA: A dataset for subseasonal forecasting and benchmarking. *Advances in Neural Information Processing Systems*, 36: 7960–7992.

Nearing, G.; Cohen, D.; Dube, V.; Gauch, M.; Gilon, O.; Harrigan, S.; Hassidim, A.; Klotz, D.; Kratzert, F.; Metzger, A.; et al. 2024. Global prediction of extreme floods in ungauged watersheds. *Nature*, 627(8004): 559–563.

Nie, Y.; Nguyen, N. H.; Sinthong, P.; and Kalagnanam, J. 2023. A Time Series is Worth 64 Words: Long-term Forecasting with Transformers. In *The Eleventh International Conference on Learning Representations*.

Papée, H. M.; and Montefinale, A. 1961. Chemical Composition of Precipitable Water Vapour over the United States. *Nature*, 191(4784): 136–138.

Qiu, X.; Hu, J.; Zhou, L.; Wu, X.; Du, J.; Zhang, B.; Guo, C.; Zhou, A.; Jensen, C. S.; Sheng, Z.; et al. 2024. TFB: Towards Comprehensive and Fair Benchmarking of Time Series

Forecasting Methods. *Proceedings of the VLDB Endowment*, 17(9): 2363–2377.

Rivero, C. R.; Patiño, H. D.; and Pucheta, J. A. 2015. Short-term rainfall time series prediction with incomplete data. In *2015 international joint conference on neural networks (IJCNN)*, 1–6. IEEE.

Roque, L.; Cerqueira, V.; Soares, C.; and Torgo, L. 2025. Cherry-picking in time series forecasting: How to select datasets to make your model shine. In *Proceedings of the AAAI Conference on Artificial Intelligence*, volume 39, 20192–20199.

Stitsyuk, A.; and Choi, J. 2025. xPatch: Dual-Stream Time Series Forecasting with Exponential Seasonal-Trend Decomposition. In *Proceedings of the AAAI Conference on Artificial Intelligence*, volume 39, 20601–20609.

Tang, Y.; Zhou, J.; Pan, X.; Gong, Z.; and Liang, J. 2023. PostRainBench: A comprehensive benchmark and a new model for precipitation forecasting. *arXiv preprint arXiv:2310.02676*.

Wan, M.; Su, Q.; Hao, H.; Wang, J.; Cui, Y.; Bi, Y.; Cao, R.; Shi, P.; Wang, Y.; Qiu, Z.; et al. 2025. PPDformer: Channel-Specific Periodic Patch Division for Time Series Forecasting. In *ICASSP 2025-2025 IEEE International Conference on Acoustics, Speech and Signal Processing (ICASSP)*, 1–5. IEEE.

Wang, S.; Li, J.; Shi, X.; Ye, Z.; Mo, B.; Lin, W.; Ju, S.; Chu, Z.; and Jin, M. 2025a. Timemixer++: A general time series pattern machine for universal predictive analysis.

Wang, S.; Wu, H.; Shi, X.; Hu, T.; Luo, H.; Ma, L.; Zhang, J. Y.; and ZHOU, J. 2024a. TimeMixer: Decomposable Multiscale Mixing for Time Series Forecasting. In *The Twelfth International Conference on Learning Representations*.

Wang, Y.; Liu, Y.; Duan, X.; and Wang, K. 2025b. Filterts: Comprehensive frequency filtering for multivariate time series forecasting. In *Proceedings of the AAAI Conference on Artificial Intelligence*, volume 39, 21375–21383.

Wang, Y.; Wu, H.; Dong, J.; Qin, G.; Zhang, H.; Liu, Y.; Qiu, Y.; Wang, J.; and Long, M. 2024b. TimeXer: Empowering Transformers for Time Series Forecasting with Exogenous Variables. In *The Thirty-eighth Annual Conference on Neural Information Processing Systems*.

Wu, H.; Hu, T.; Liu, Y.; Zhou, H.; Wang, J.; and Long, M. 2023. TimesNet: Temporal 2D-Variation Modeling for General Time Series Analysis. In *The Eleventh International Conference on Learning Representations*.

Wu, H.; Xu, J.; Wang, J.; and Long, M. 2021. Autoformer: Decomposition transformers with auto-correlation for long-term series forecasting. *Advances in neural information processing systems*, 34: 22419–22430.

Yin, W.; Zhou, C.; Zhou, F.; Tian, Y.; Yang, X.; Wang, X.; Tian, R.; Xiao, Y.; Zhang, W.; Kong, J.; and Yao, Y. 2024. A Lightning Nowcasting Model Using GNSS PWV and Multi-source Data. *IEEE Transactions on Geoscience and Remote Sensing*, 62: 1–10.

Zeng, A.; Chen, M.; Zhang, L.; and Xu, Q. 2023. Are transformers effective for time series forecasting? In *Proceedings of the AAAI conference on artificial intelligence*, volume 37, 11121–11128.

Zhang, Y.; Long, M.; Chen, K.; Xing, L.; Jin, R.; Jordan, M. I.; and Wang, J. 2023. Skilful nowcasting of extreme precipitation with NowcastNet. *Nature*, 619(7970): 526–532.

Zhou, H.; Zhang, S.; Peng, J.; Zhang, S.; Li, J.; Xiong, H.; and Zhang, W. 2021. Informer: Beyond efficient transformer for long sequence time-series forecasting. In *Proceedings of the AAAI conference on artificial intelligence*, volume 35, 11106–11115.